Improved Polypropylene Thermoformability through Polyethylene Layering

Jordan, Alex
Meyer, Laryssa
Kim, Kyungtae
Lee, Bongjoon
Bates, Frank
Macosko, Chris

To be published in: ACS Applied Materials & Interfaces

DOI to publisher's version: 10.1021/acsami.2c08586

ACS APPLIED MATERIALS & INTERFACES

www.acsami.org

Research Article

Improved Polypropylene Thermoformability through Polyethylene Layering

Alex M. Jordan,* Laryssa Meyer, Kyungtae Kim, Bongjoon Lee, Frank S. Bates, and Christopher W. Macosko

Cite This: https://doi.org/10.1021/acsami.2c08586

Read Online

ACCESS | Metrics & More | Article Recommendations | Supporting Information

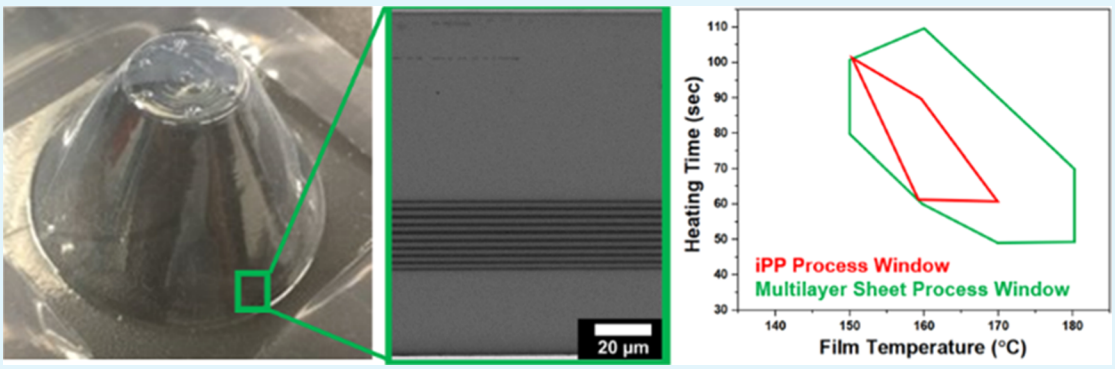

ABSTRACT: Due to its low cost, stiffness, and recyclability, isotactic polypropylene (iPP) is an excellent candidate for packaging applications. However, iPP is notoriously difficult to thermoform due to its low melt strength. The addition of just 10 thin layers of high-molecular-weight, linear low-density polyethylene (LLDPE) into iPP sheets by coextrusion significantly increased extensional viscosity and reduced sag. Both LLDPE and iPP were metallocene-catalyzed with excellent adhesion as measured in our previous work. We performed a series of hot tensile tests and sheet sag measurements to determine the properties of the iPP sheet and the multilayer sheet between 130 and 180 °C. To evaluate the thermoformability of these multilayer sheets, truncated conical cups were positive vacuum formed at different temperatures and heating times, and the crush strength was measured. Cups that released easily from the mold with good shape retention and a crush strength within 80% of the maximum value were used to define a temperature−time thermoformability window. We estimated the maximum stress that occurred during the thermoforming process to be 5 MPa. Layer thicknesses before and after thermoforming were used to estimate an average strain of 0.78. The thin LLDPE layers decreased the yield stress below 5 MPa. This enabled thermoforming at sheet temperatures as low as 150 °C. The immiscible LLDPE interfaces increased extensional viscosity, which decreased sag in the multilayer sheets compared to iPP. This broadened the thermoforming range to temperatures as high as 180 °C and allowed longer heating times. These highly thermoformable, layered sheets may be recycled as iPP since they contain only 8% of LLDPE.

KEYWORDS: *polyolefins, thermoforming, process analysis, multilayer coextrusion, polymer mechanics*

1. INTRODUCTION

The global market for thermoformed packaging was $41B in 2019 and is expected to grow by 5.1% per year through 2027.[1] Due to its low cost, mechanical properties, and recyclability, isotactic polypropylene (iPP) is an excellent candidate for packaging applications. However, iPP is notoriously difficult to thermoform due to its low melt strength. Some applications use high-molecular-weight (low melt index; MFI) iPP for thermoforming;[2] however, low MFI requires larger extruders, more energy, and often decreases extruder output to compensate for higher operating pressure. Lau and colleagues have shown that as the zero-shear viscosity of iPP increases, the extent of sagging before thermoforming decreases.[3] Macauley et al. demonstrated that incorporating nucleating agents improves the thermoformability and extensional processing features of iPP.[4] It is well known that long-chain branching induces strain hardening in iPP melts, making long-chain branched iPP suitable for thermoforming.[5−8] A number of researchers have utilized reactive extrusion to create long-chain branched iPP to improve thermoformability.[9,10] Specifically, Münstedt and colleagues correlated the improved thermoformability to strain hardening behavior recorded during transient extensional viscosity measurements.[9] Yamaguchi and Suzuki observed similar improved thermoformability

Received: May 14, 2022
Accepted: June 28, 2022

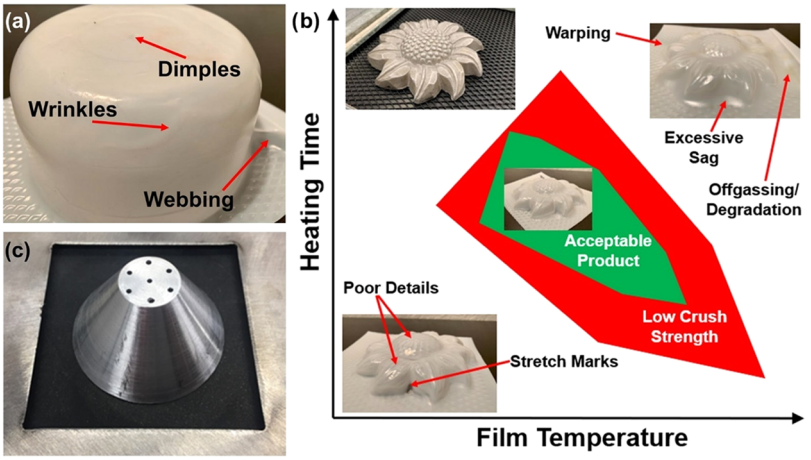

Figure 1. (a) Thermoforming defects that result from poor mold design; (b) a sunflower mold used to visualize the processing window for an HDPE sheet; and (c) form used to produce the truncated cone for crush testing.

with blends of high-density polyethylene (HDPE) and cross-linked HDPE.[11]

In previous work, we achieved increased extensional viscosity and strain hardening in iPP melts by exploiting the interfacial tension that exists in multilayer polyolefin sheets.[12] As the multilayer sheet is elongated, interfacial tension resists the creation of more interfacial area leading to observable strain hardening. Additionally, we probed the interfacial properties between films of various iPP and polyethylene grades and found excellent adhesion and mechanical properties when a metallocene-catalyzed iPP was combined with a metallocene-catalyzed linear low-density polyethylene (LLDPE).[13−15] Thus, we selected a metallocene-catalyzed iPP and LLDPE to fabricate a multilayer sheet to be thermoformed. While HDPE/iPP had a slightly higher interfacial tension than LLDPE/iPP, the adhesion strength was more than an order of magnitude lower in the HDPE/iPP system,[13] which could possibly lead to premature failure during compression testing. Adding just 10 thin layers of high-molecular-weight LLDPE into an iPP sheet via coextrusion allowed thermoforming at lower and higher temperatures than a simple iPP sheet. Coupled with improvements in barrier properties that Baer and colleagues observed in polyolefin multilayer sheets,[16] as well as other multilayer systems,[17,18] this work represents a potential route to improved iPP packaging.

2. EXPERIMENTAL SECTION

2.1. Materials. Two polyolefins were used in this study: iPP (Total, Lumicene MH04yN9, MFI 4.0 g/10 min) and LLDPE (Total, Lumicene M1810EP, MFI 0.9 g/10 min). Both polyolefins were synthesized using a metallocene catalyst, which results in a relatively narrow molecular weight distribution, minimal oligomer content, and excellent adhesion between the two immiscible polyolefins.[13]

2.2. Sheet Fabrication. Multilayer coextrusion was used to produce a continuous sheet of iPP and LLDPE. Fabrication of iPP/LLDPE multilayer sheets using coextrusion has been described elsewhere.[13,19,20] A single-screw extruder (25 mm diameter, Killion) was fed with LLDPE, while a second twin-screw extruder (16 mm diameter, Prism TSE 16TC) was fed with iPP. Each extruder was connected to a metered gear pump to control the final volume composition of each sheet, which was 8% LLDPE and 92% iPP with 10 LLDPE layers alternating with 11 iPP layers for a total of 21 layers. The volume composition was chosen to minimize the amount of LLDPE in the final sheet, while still allowing the gear pumps to operate reliably. The multilayer sample, designated as $iPP_{92}/LLDPE_8$, had a final cross section of 78 mm × 0.4 mm after leaving a 150 mm wide coat hanger manifold die and being drawn down in a three-roll stack held at 25 °C. A constant processing temperature of 180 °C was used for both extruders, gear pumps, feedblock, layer multipliers, and the die.

2.3. Thermoforming. Sheets were thermoformed using a truncated cone with a top diameter of 12.7 mm and a bottom diameter of 38.1 mm at a 60° vertex angle (α), as illustrated in Figure 1c. The location and size of vent holes are shown in Figure S2. Sheets were placed in an aluminum holder, clamped on all four edges, and the truncated cone was formed by pressing the cone upward into the heated sheet before applying 16.25 kPa of vacuum pressure to draw the sheet downward to the form (Formech 300XQ) using a range of sheet temperatures (140−180 °C) and heating times (40−120 s). Formed sheets were left on the mold to cool for 60 s before being removed. At least 48 h were allowed to pass before the cones were compression-tested.

Sheet temperature heating profiles were measured using a FLUKE infrared camera. Temperature measurements were collected in triplicate for each combination of heater power settings. To achieve the desired sheet temperatures, five combinations of heater power settings were used on the Formech 300XQ. Four of the settings used heating zones 1, 3, and 4 set to either 70, 75, 85, or 100%; these four settings resulted in measured sheet surface temperatures of approximately 150, 160, 170, and 180 °C. The fifth heater setting employed only zones 1 and 3 set to 100% power, which resulted in a sheet surface temperature of approximately 140 °C. Heat transfer calculations (see the Supporting Information) indicate that temperature gradients across the thin sheet can be ignored. Temperatures measured during heating are shown in Figure S2. All sheets were at the indicated temperature after a 40 s heating time.

There are a number of defects that may occur during the thermoforming process. Some defects, such as wrinkles, webbing, and dimples (Figure 1a), are the result of poor mold design.[21] Other defects like poorly defined details and stretch marks result from the elastic modulus of the sheet being too high. Since the elastic modulus is temperature-dependent, these issues can be resolved by increasing the sheet temperature, but high temperatures can lead to sagging or off-gassing when the material degrades. Warping and sagging occur when the modulus of the material is not sufficient to support its own weight during heating and can be remedied by decreasing the sheet temperature or heating time (Figure 1b). For this study, we performed a quick screening to determine a range of sheet temperatures and heating times that produced a visually acceptable part with no observable defects. These conditions are schematically identified as the red and green zones in Figure 1b. We then performed crush strength tests to screen for "acceptable parts" (green zone,

https://doi.org/10.1021/acsami.2c08586
ACS Appl. Mater. Interfaces XXXX, XXX, XXX−XXX

Figure 1b). These criteria and the crush strength of the truncated cones (Figure 1c) were used to determine a processing window.

2.4. Crush Strength. To characterize whether the cone produced at each set of conditions was acceptable we measured the crush force required to buckle the cone. The crush force, F_{cr}, can be related (eq 1) to the elastic modulus (E) and Poisson's ratio (μ) of the material, along with the wall thickness (h), by a constant (γ), which is ~0.33 if $10° < \alpha < 75°$.[22]

$$F_{cr} = \gamma \frac{2\pi E h^2 \cos^2(\alpha)}{\sqrt{3(1-\mu^2)}} \quad (1)$$

Crush strength is sensitive to wall thickness since F_{cr} of a truncated cone is proportional to h^2, i.e., a decrease of 20% in F_{cr} indicates a decrease in the local minimum wall thickness of ~10%.[22] The maximum crush strength ($F_{cr,max}$) for each sample type was directly measured between compression plates (MTS, QTest 50LP). Successful thermoforming conditions were characterized as any combination of heating time/sheet temperature that produced a cone with $>0.8F_{cr,max}$. A minimum of five samples were tested for each combination of sheet temperature and heating time settings.

2.5. Dynamic Mechanical Analysis. Dynamic mechanical analysis (DMA, TA Q800) temperature sweeps were performed on LLDPE and iPP control sheets as well as the $iPP_{92}/LLDPE_8$ multilayer sheet. Sheets were cut into rectangular sections (6.25 mm width × 25 mm length) and placed in a furnace. The gauge length was 15 mm with a 15 μm amplitude deformation at a frequency of 1 Hz. The temperature was increased from 30 to 140 °C for the LLDPE control and from 30 to 175 °C for the iPP control and the $iPP_{92}/LLDPE_8$ multilayer sheet at a heating rate of 3 °C/min.

2.6. Extensional Rheology. Extensional rheology was performed using the Extensional Viscosity Fixture (EVF) on a TA Instruments ARES-G2 rheometer. The extruded samples were cut into 18 mm × 5 mm × 0.5 mm rectangles for extensional testing. Before starting the measurements, samples were held in the EVF at 180 °C for 10 s and monitored with a video camera to ensure that sagging or shrinking did not occur. All extensional rheology measurements were performed at 180 °C with an extension rate of 5 s^{-1} at least three times. The strain direction was parallel to the extrusion direction of the sample. The multilayer transient extensional viscosity ($\eta^+_{E,M}$) was fit based on the extensional viscosity of each component, $\eta^+_{E,PE}$ and $\eta^+_{E,PP}$, the associated interfacial tension, Γ, and the melt volume ratio of LLDPE/iPP (ϕ) (eq 2).[12] Other terms in the fitting equation include the number of layers (N), strain rate ($\dot{\varepsilon}$), initial multilayer sheet thickness (H_0), and stretching time (t). The value for Γ was taken as 0.8 mN/m, whereas N was counted from scanning electron microscopy (SEM) images.[12]

$$\eta^+_{E,M}(t) = \left(\frac{\phi}{\phi+1}\right)\eta^+_{E,PE}(t) + \left(\frac{1}{\phi+1}\right)\eta^+_{E,PP}(t) + \frac{\Gamma(N-1)}{\dot{\varepsilon}H_0 e^{(-\dot{\varepsilon}t/2)}} \quad (2)$$

2.7. Scanning Electron Microscopy (SEM). The coextruded multilayer iPP/LLDPE samples were cryo-microtomed at −120 °C with a glass knife to expose a smooth edge-on cross section of the multilayer sheet. Each sample was cryo-microtomed at an angle so that the knife marks were clearly distinguishable from the multilayer structure. The trimmed iPP/LLDPE multilayer cross section was exposed to the vapors of a 0.5% ruthenium tetroxide (RuO_4) solution in a 10 mL vial for 30 min before being dried overnight in a ventilated fume hood. Additional trimming was performed by cryo-microtoming at −120 °C with a glass knife to remove excess RuO_4 aggregates on the surface. Following the second trimming, 0.56 nm of iridium was sputter-coated (Leica EM ACE600) on the cryo-microtomed surface to prevent charging during SEM imaging. The SEM instrument (Hitachi SU8230) was equipped with a cold field emission gun, and the SEM images were obtained with an accelerating voltage of 25 kV. Due to the different staining rates between LLDPE and iPP by RuO_4, the iPP/LLDPE multilayer structure was clearly observed with a back-scattered electron detector (BSE) where iPP and LLDPE layers are distinguished as bright and dark domains, respectively.

2.8. Estimating Stress, Strain, and Strain Rate in the Thermoforming Process. Measuring the individual layer thickness before and after the thermoforming process provides an estimate of local strain experienced in the sheet during the thermoforming process. Assuming an affine deformation, the final layer thickness (H_f) is related to the initial thickness (H_0) and strain (ε) (eq 3).

$$\varepsilon = -2\left[\ln\left(\frac{H_f}{H_0}\right)\right] \quad (3)$$

Videos obtained during thermoforming provided for the estimation of the average elongational strain rate during processing (Figure S3). Along with measuring strain within the sheet, and assuming affine deformation along with the known mold geometry and process conditions, the applied stress can be deduced at various locations during the thermoforming process. The average strain in all layers was 0.8, the strain rate was ~26 s^{-1}, and a maximum stress of ~5.1 MPa was estimated to occur at the top ridge of the cone, as described in the Supporting Information.

2.9. Uniaxial Tensile Testing. Tensile testing (TA Q800) was carried out at temperatures ranging from 130 to 150 °C. Sheets were cut into rectangular pieces (2 mm width × 15 mm length × 0.4 mm thick) and loaded into the furnace with an initial gauge length of 6 mm. Samples were held isothermally at 130−160 °C for 5 min before extension at a rate of 6 mm/min. This translates to a strain rate of ~0.02 s^{-1} At least three samples were tested at each temperature. While this strain rate is 3 orders of magnitude lower than that experienced during thermoforming, the yield strain of iPP is not strongly rate-dependent.[23] Ebert and colleagues modeled and experimentally determined the yield stress of iPP to be ~25 MPa at a rate of 0.0115 s^{-1} and ~40 MPa at a rate of 11.5 s^{-1}.[23] The yield stresses measured at elevated temperatures for our samples were all <8 MPa; as a result, the measured yield stress at this slower testing speed is a reasonable approximation of the stresses experienced during thermoforming at higher deformation rates.

2.10. Sag Deflection. The extent of sag was measured as a function of heating times at sheet temperatures ranging from 160 to 180 °C. A grid of 1 cm × 1 cm squares was drawn on the iPP control and $iPP_{92}/LLDPE_8$ sheets prior to being placed under the heating element to help visualize the extent of sag. Photographs of the grid were taken during heating to visualize sag. Deflection at the center of the sheet was measured using a pair of Mitutoyo calipers. The sag deflection was measured at 10 s intervals. Sag deflection experiments were repeated in triplicate at each of the three temperatures tested.

3. RESULTS AND DISCUSSION

3.1. DMA. Both polyolefin control samples were screened for thermoformability using a DMA temperature sweep. Throne qualitatively describes a gradual decrease in E' with increasing temperature as a screening tool that indicates a material is suitable for thermoforming.[21] However, there were no quantified values to accompany this consideration. While studying heat sealing of polyolefins, Stehling and Meka identified a "semimelt" region, E' between 10 and 100 MPa, for optimum sealing. Temperatures corresponding to this modulus range allowed sufficient molecular mobility on the microscale during heat sealing while still maintaining dimensional stability on the macroscopic scale.[24] In Figure 2, 10 MPa $< E' <$ 100 MPa is indicated as the semimelt region, which was used to quantify a temperature range for the decrease in E'. Because of its low crystallinity and high molecular weight, the LLDPE control exhibited a very gradual decrease in E' with temperature; LLDPE remained in the semimelt state between temperatures of 60 and 108 °C, suggesting a forming window of 48 °C. In contrast, the iPP control exhibited a very sharp

https://doi.org/10.1021/acsami.2c08586
ACS Appl. Mater. Interfaces XXXX, XXX, XXX−XXX

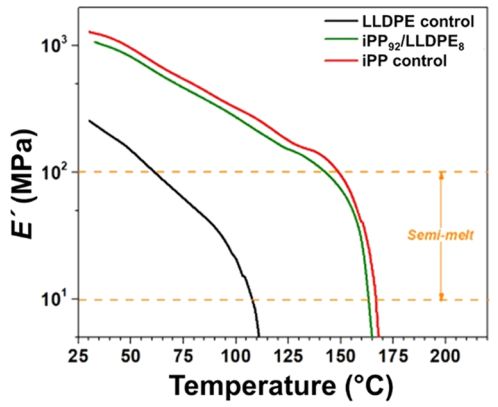

Figure 2. DMA temperature sweep of LLDPE and iPP control sheets as well as the $iPP_{92}/LLDPE_8$ multilayer sheet.

decrease in E' after passing through the melting temperature, T_m, due to its narrow molecular weight distribution and high crystallinity; iPP remained in the semimelt state between temperatures of 149 and 167 °C, only 18 °C.

3.2. Thermoforming of Controls. As expected from the DMA results, and born out in Figure 3a, the window for successful thermoforming of iPP was quite narrow. The highest F_{cr} recorded was 23.2 ± 2.9 N at a sheet temperature of 160 °C with a heating time of 90 s. While the sheet temperature of 140 °C nominally produced a cone, the edges of the cone at the base were not well-defined due to the stiffness of iPP at that temperature. When heated to a temperature of 180 °C, there was excessive sheet sagging in the iPP control due to its low melt strength; this prevented the instrument from pulling a full vacuum, and as a result, the cup walls were highly uneven; walls at the base of the cone ranged in thickness from 0.12 to 0.16 mm, while walls at the top of the cone ranged in thickness from 0.09 to 0.14 mm. While F_{cr} was measured for these conditions, the bars in Figure 3a are color-coded white to match the scheme shown in Figure 1b due to the obvious distortion in wall thickness. Based on the $0.8F_{cr,max}$ cutoff, there were six sets (including that maximum strength set) of processing conditions that produced an acceptable cone (Figure 3). The wall thickness at the base of these acceptable cones ranged from 0.13 to 0.15 mm while walls at the top of these cones ranged in thickness from 0.11 to 0.13 mm.

Figure 3b shows F_{cr} vs heating time and temperature for LLDPE. As expected, virtually every combination of sheet temperature (140−180 °C) and heating times (40−120 s) produced a cone with no visual defects. However, the flexibility and low stiffness of LLDPE resulted in measured F_{cr} values <7 N. Of the 45 processing conditions screened during the thermoforming experiments, 30 combinations of film temperature and heating time produced a cone with $F_{cr} > 0.8F_{cr,max}$. While this meets the previously defined criteria for successful thermoforming, the flexibility and tackiness of the LLDPE caused difficulties with demolding. Moreover, the low stiffness of LLDPE is prohibitive for any type of protective rigid packaging application.

3.3. Multilayer Polyolefin Thermoforming. The multilayer sheet ($iPP_{92}/LLDPE_8$) was also screened for thermoformability using DMA (Figure 2). Given that the $iPP_{92}/LLDPE_8$ is a majority iPP, it is not surprising that the trend of E' as a function of temperature closely follows that of the iPP control. The $iPP_{92}/LLDPE_8$ multilayer film remains in the semimelt state between temperatures 142 and 162 °C, a 20 °C

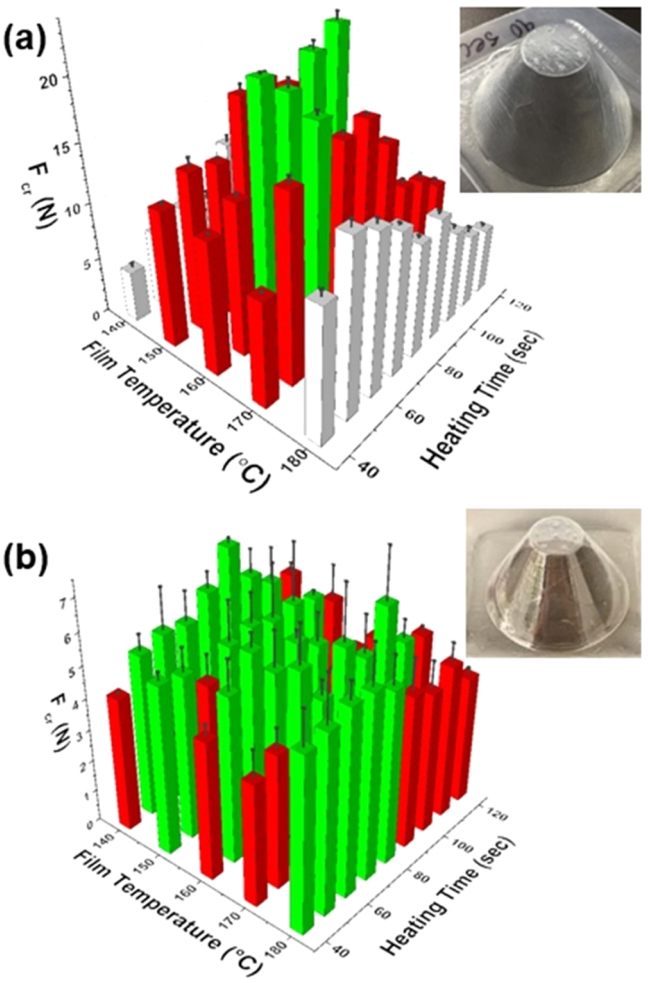

Figure 3. Thermoforming process window results for (a) iPP control and (b) LLDPE control. Green bars indicate F_{cr} values ≥ $0.8F_{cr,max}$; red bars indicate F_{cr} values < $0.8F_{cr,max}$; and white bars indicate a cone with observable visual defects. The inset images that accompany each data set show a picture of the thermoformed cup fabricated from each material.

range. Thus, by DMA alone, we would expect $iPP_{92}/LLDPE_8$ to have a narrow processing window similar to the iPP control. Surprisingly, the thermoforming window was much broader for the $iPP_{92}/LLDPE_8$ multilayer sheet.

An identical series of heating time and sheet temperature thermoforming experiments were performed with truncated cones of $iPP_{92}/LLDPE_8$ sheets. Figure 4 shows results in sharp contrast with the iPP control. The maximum F_{cr} of the $iPP_{92}/LLDPE_8$ samples was 21.1 ± 1.9 N, which was produced with a sheet temperature of 160 °C and a heating time of 80 s. Taking the maximum F_{cr} of each component material, a volume additive model predicts that 21.9 N for the crush strength of the $iPP_{92}/LLDPE_8$ sample, in good agreement with the experimentally determined value. Unlike the iPP control, there were 20 sets of heating times and sheet temperatures that produced a cone with F_{cr} > 16.9 N ($0.8F_{cr,max}$). Thus, the thermoforming behavior of the $iPP_{92}/LLDPE_8$ is far more forgiving than that of the iPP control. From a practical processing standpoint, the 10 s reduction in heating time represents an 11% decrease in overall cycle time. Also worth noting is that acceptable structures were formed at a sheet

https://doi.org/10.1021/acsami.2c08586
ACS Appl. Mater. Interfaces XXXX, XXX, XXX−XXX

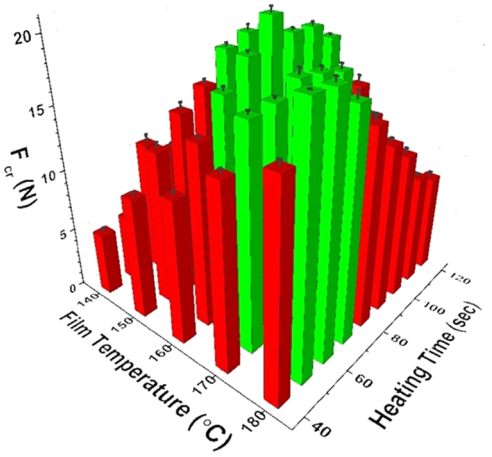

Figure 4. Thermoforming process window for $iPP_{92}/LLDPE_8$ multilayer sheet. Green bars indicate F_{cr} values $\geq 0.8F_{cr,max}$, and red bars indicate F_{cr} values $< 0.8F_{cr,max}$.

temperature of 180 °C, where the iPP sagged excessively producing unacceptable parts.

To be used for barrier packaging, the layers in a multilayer structure should remain intact. We anticipated little to no layer breakup due to good adhesion between the iPP and LLDPE materials in our previous work.[13] Figure 5 shows SEM images of the multilayer sheets. Light gray represents iPP domains, while the dark contrast regions correspond to LLDPE layers. The SEM image in Figure 5b was taken of a sheet prior to thermoforming. It is clear that the multilayer integrity is excellent with 21 individual layers present. From image analysis, 92% of the sheet, by volume, is iPP. Before thermoforming, the layer structure within the sheet was well defined (Figure 5b). Cross-sectional SEM images were obtained of the thermoformed cone (160 °C, 80 s) at the top (Figure 5c) and bottom (Figure 5d) ridges. Examination of these images revealed no damage to the layered structure during the heating and stretching processes associated with thermoforming. As a result, we can rule out layer breakup as the explanation for this process improvement and must search for a more fundamental understanding of the thermoforming process.

3.4. Thermoforming Analysis. We carry out a simple analysis of the thermoformability of our polyolefin sheets by estimating the maximum stress and strain that they experience in the process. To estimate the local strain throughout the thickness of the sheet, we assume affine deformation and calculate the local Hencky strain in each iPP layer (Figure 6a) and LLDPE layer (Figure 6b). There are three principal observations to draw from this analysis.

First, it is clear in Figure 6 that the LLDPE layers are drawn down more than the iPP layers. The average Hencky strain is 0.95 in the LLDPE layers, but only 0.54 in iPP. This is understandable since the LLDPE is fully molten at 160 °C, while the iPP is near its melting point. Second, the local Hencky strain in the LLDPE layers is larger near the free surface than at the surface of the film that contacts the mold. This also makes sense as the layers in closer contact with the cold metal mold will cool rapidly upon contacting the mold while the layers in contact with air will cool slower and remain

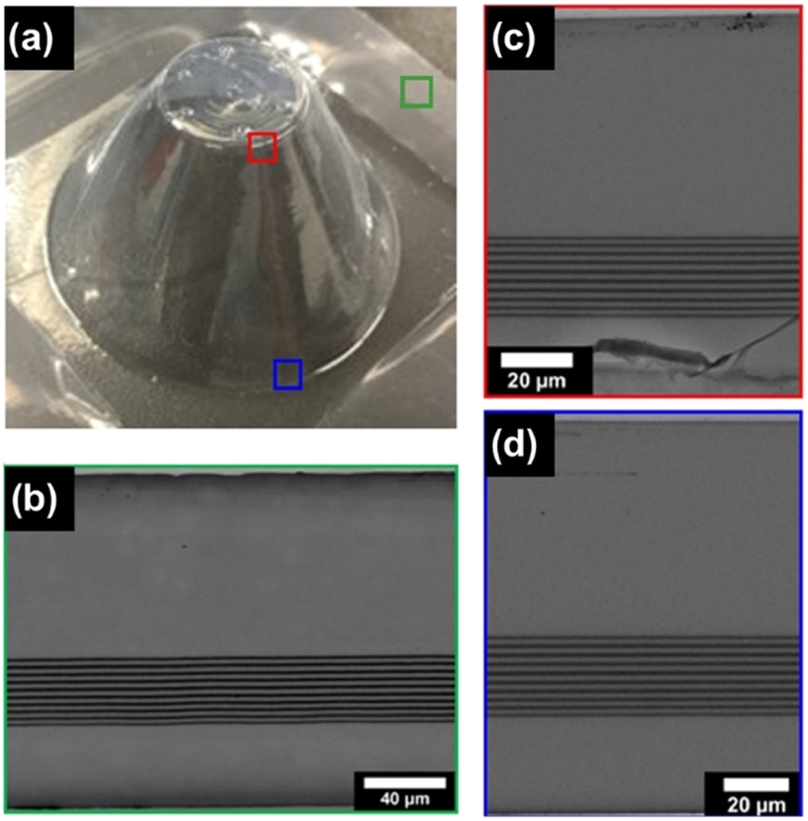

Figure 5. (a) Thermoformed cone from multilayer sheet. Cross-sectional SEM images of the (b) undeformed (green outline) multilayer sheet and after thermoforming at the (c) top (red outline) and (d) base (blue outline) of the thermoformed cone. The thin iPP layer at the bottom of each SEM image (b–d) was the layer in contact with the aluminum mold during thermoforming.

https://doi.org/10.1021/acsami.2c08586
ACS Appl. Mater. Interfaces XXXX, XXX, XXX−XXX

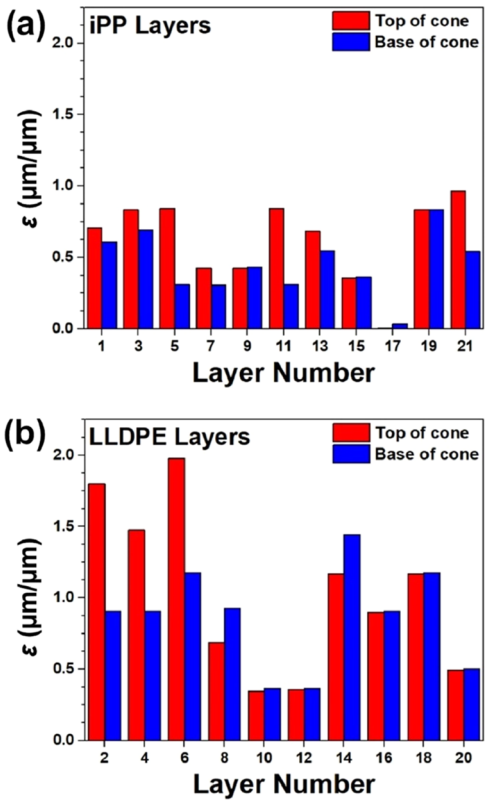

Figure 6. Local Hencky strain estimates in each iPP (a) and LLDPE (b) layer at the top and bottom of the thermoformed multilayer cone. Layer 21 is the iPP layer in contact with the mold. Layer 20 is the LLDPE layer next to it.

molten longer, allowing them to absorb the deformation and stretch further than the frozen layers. Third, the local Hencky strain appears to be higher at the top of the cone than at the base, especially near the free surface of the sheet (lower layer number). This result is somewhat unexpected for the drape thermoforming process. During vacuum thermoforming (negative forming), thinner walls would be expected at the top of the cone as it is drawn down into the mold. During drape thermoforming (positive forming), thinner walls would be anticipated at the base of the cone as the sheet is stretched down over the mold.[25,26] These strain measurements suggest that the sheet may be slipping over the top surface of the cone and the wall of the entire part is being elongated.

Aside from these trends, we average all of the local Hencky strain measurements leading to an estimated average strain of 0.78 occurring throughout the sheet during thermoforming with this particular mold. Video-recorded motion studies (Figure S3) of the thermoforming process revealed that the deformation occurred over a time span of ~0.03 s, suggesting that the strain rate is ~26 s^{-1}.

Knowing the dimensions of the cone and applied vacuum pressure provides the approximate stress within the walls of the cone during thermoforming. The local stress was estimated as 5.1 MPa at the top ridge of the cone and 1.7 MPa at the base of the cone (see the Supporting Information). It should be noted that these estimates are based on assumptions satisfied during vacuum forming, but there may be some additional stress induced by punching the form up into the molten sheet. From these estimates, we have bounds for the thermoforming process with this mold. These suggest that the material must elongate further than a strain of 0.78 and be deformable at stresses lower than 5.1 MPa when deformed at a strain rate of ~26 s^{-1} at a given temperature. Figure 7 and Table S1 show the tensile test results for iPP and the multilayer sheets with the strain and stress bounds overlaid.

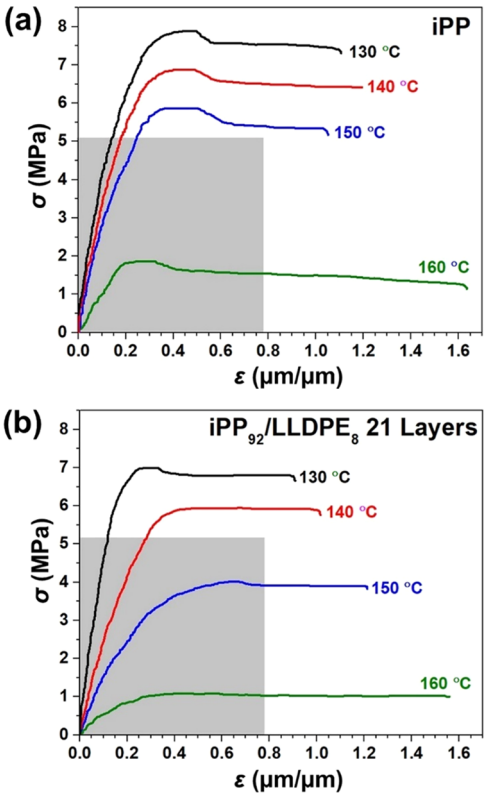

Figure 7. Uniaxial tensile data for the iPP control sheet (a) and the multilayer sheet (b) at temperatures of 130−160 °C. The gray box indicates average strain achieved and maximum stress applied during the thermoforming process.

Tensile testing of the iPP control (Figure 7a) at elevated temperatures revealed that σ_y at temperatures ≤ 150 °C was above the maximum stress exerted during the thermoforming process. This suggests that the sheet is too rigid at lower temperatures to be thermoformed. Tensile testing of the iPP control revealed only one temperature, 160 °C, that met the criteria outlined for successful forming with the equipment used in this study. This correlated well with the observed thermoforming behavior (Figure 3), revealing that 160 °C was the optimal temperature for thermoforming; four of the six acceptable processing conditions occurred at 160 °C (60−90 s heating time). However, it is worth noting that the cone produced at a sheet temperature of 150 °C and heating time of 100 s met the acceptability criteria.

Upon layering LLDPE into iPP, the sheet became slightly more ductile at elevated temperatures (Figure 7b). While the yield stress (σ_y) at 130 and 140 °C exceeds 5.1 MPa, after being heated to 150 °C, the σ_y of the sheet is 4.1 ± 0.5 MPa. When thermoforming the multilayer sheet at 150 °C, all heating times 80−100 s produced an acceptable cone. The decrease in σ_y is expected as ductile LLDPE is added into the iPP sheet. Here, we note that the large strain tensile experiments simulate the thermoforming process more than

https://doi.org/10.1021/acsami.2c08586
ACS Appl. Mater. Interfaces XXXX, XXX, XXX−XXX

the small-amplitude deformation ($\varepsilon \sim 0.001$) experiments carried out in the DMA (Figure 2).

The iPP control was not able to form a visually acceptable cone at temperatures ≤ 150 °C ($\sigma_y = 6.4 \pm 0.8$ MPa), while the $iPP_{92}/LLDPE_8$ sheet was not able to form a visually acceptable cone at temperatures ≤ 140 °C ($\sigma_y = 5.8 \pm 0.9$ MPa). This implies that the actual stress of the drape forming process may be closer to ∼6 MPa, roughly ∼20% higher than our estimate based on a simple vacuum forming process. While our estimate of σ_{max} is not exact, it is an approximation that is sufficiently close to be used as a screening tool before mold production and testing of the drape forming process.

In tensile testing, neither the iPP control nor $iPP_{92}/LLDPE_8$ multilayered sheets were able to consistently withstand the gravitational weight of the fixture when heated above T_m, so transient extensional rheology measurements were taken as a substitute at 180 °C. Notably, the η_E^+ of the LLDPE control was ∼4× higher than that of the iPP control at 180 °C (Figure 8). Using a strain of 0.8 ($t = 0.16$ s) as a comparison point, the

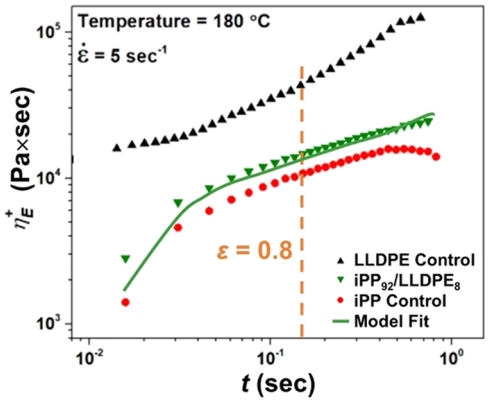

Figure 8. Transient extensional viscosity of both control sheets and the multilayer sheet. Data from iPP and LLDPE controls were used in our previously developed model[12] to predict (solid green line) the transient extensional viscosity of the multilayer film.

η_E^+ of the LLDPE control was 4.35×10^4 Pa·s, while the η_E^+ of the iPP control was 1.07×10^4 Pa·s. The η_E^+ of the $iPP_{92}/LLDPE_8$ multilayer was 1.45×10^4 Pa·s; our previously developed model to describe η_E^+ of multilayer systems predicted η_E^+ of 1.35×10^4 Pa·s, in good agreement with the experimental data. The solid line in Figure 8 shows that our model describes the η_E^+ of the $iPP_{92}/LLDPE_8$ multilayer sheet accurately over a wide strain range.[12] Although the improvement in η_E^+ achieved through layering appears minimal in Figure 8, it constitutes a 36% improvement compared to the iPP control at $\varepsilon = 0.8$. While the iPP control could not be successfully thermoformed at 180 °C, all heating times between 70 and 90 s produced acceptable products using the $iPP_{92}/LLDPE_8$ multilayer sheet at 180 °C. This result highlights the value of extensional rheology measurements in gaining a better understanding of the thermoforming process.

While transient extensional measurements were taken at a rate of 5 s^{-1}, approximating the stretching process, the heating stage is characterized by a low strain rate as the sheet gradually sags under its own weight (Figures S6−S8). As the sheet sags, the thickness of the sheet becomes increasingly nonuniform. This is further exacerbated during the stretching during thermoforming. The locally thin walls in turn result in a decreased overall crush strength. It follows that minimizing sag is an avenue to improve thermoformability.

Figure 9 shows sag deflection vs heating time at 160, 170, and 180 °C. The first trend to note is that when comparing sag

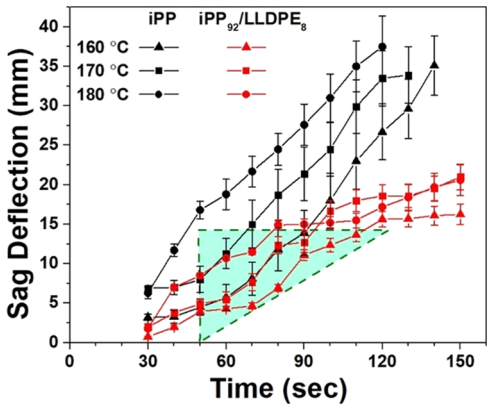

Figure 9. Sag deflection measured for iPP control and $iPP_{92}/LLDPE_8$ multilayer sheet for various heating times and temperatures. The superimposed green-shaded region denotes sheet temperatures and heating times that formed an acceptable cone for iPP control and $iPP_{92}/LLDPE_8$ multilayer sheet.

deflection, the iPP control is on average 72% greater for the same heating time and sheet temperature combinations than the $iPP_{92}/LLDPE_8$ multilayer sheets. At heating times up to 90 s with a sheet temperature of the 160 °C sag of the iPP control was less than 15 mm and was comparable to the sag of the multilayer sheet when it was heated to 180 °C. iPP cones produced at 170 °C with a heating time of 60 s also barely met the acceptability criteria with a crush force of $\sim 0.81 F_{cr,max}$; the sag deflection under these conditions was 11.3 ± 1.9 mm. In contrast, heating times of 60−110 s (160 °C), 50−90 s (170 °C), and 50−70s (180 °C) all produced acceptable cones from the $iPP_{92}/LLDPE_8$ multilayer sheet. These heating times and sheet temperatures are highlighted by a green-shaded region in Figure 9. By examining the superimposed shaded region, it appears that the heating time and sheet temperature conditions that produced an acceptable cone coincided with a sag deflection < 15 mm. This thermoforming behavior correlates well to the drastically reduced sag deflection of the multilayer sheets. In our model for extensional viscosity (eq 2), the interfacial tension contribution is divided by the strain rate, so at low strain rates, the enhancement of η_E^+ is anticipated to be even larger than that shown in Figure 8. From this, it follows that the extent of sag would be greatly reduced for the multilayer sheet.

There were six combinations of heating time and sheet temperature that produced an acceptable product using the iPP control. This increased to 17 combinations of heating time and sheet temperature that produced an acceptable product after creating a 21-layer polyolefin system with just 8% LLDPE (Figure 10a). The Association of Plastics Recyclers recommends >90% purity of either PE or PP to be "recyclable".[27] With <10% LLDPE, this layered system meets the standard for recyclability as defined by APR. The minimal addition of LLDPE also does not significantly decrease the crush strength of the cone. The $F_{cr,max}$ decreased from 23.2 ± 2.9 N in the iPP control to 21.1 ± 1.9 N in the $iPP_{92}/LLDPE_8$ multilayer system (Figure 10b).

https://doi.org/10.1021/acsami.2c08586
ACS Appl. Mater. Interfaces XXXX, XXX, XXX−XXX

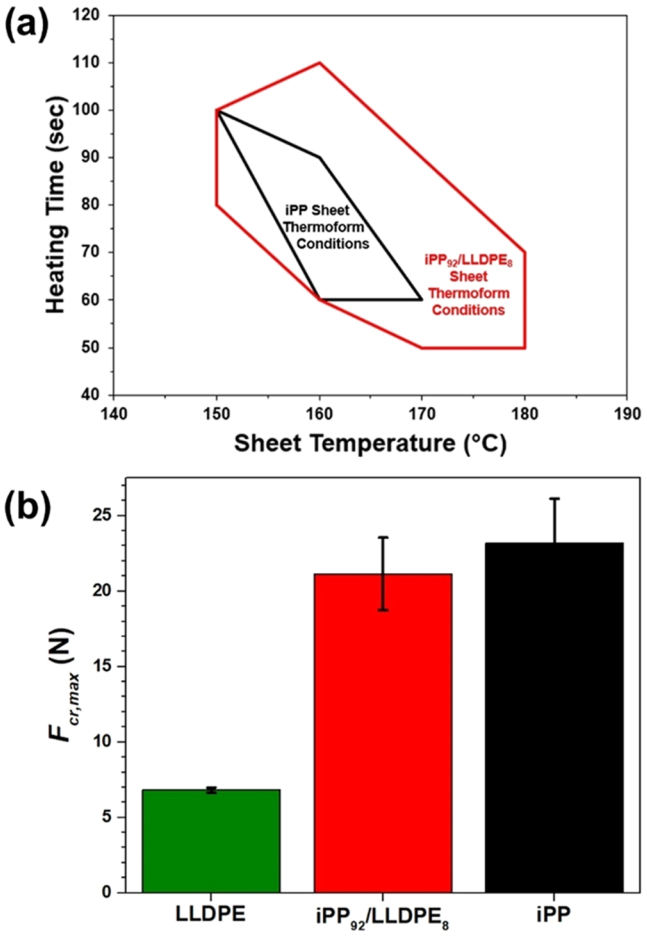

Figure 10. (a) Sheet temperatures and heating times that produced an acceptable cone from iPP control (black) and $iPP_{92}/LLDPE_8$ multilayer sheet (red). (b) $F_{cr,max}$ of thermoformed LLDPE and iPP cones as well as the thermoformed multilayer cone.

4. CONCLUSIONS

Historically, DMA has been utilized as a screening tool to assess the suitability of a material for thermoforming. While DMA may be used for quick material screening, the associated small-amplitude straining is not representative of the large deformations that occur during the thermoforming process. We found that a deeper analysis of tensile testing data at temperatures approaching the melt temperature and sag measurements above the melt temperature provide a more reliable prediction of thermoformability.

In this work, we demonstrated the difficulty of thermoforming iPP and the ease of thermoforming LLDPE. The iPP displayed a very sharp decrease in E' through the semimelt state measured by DMA, while the LLDPE displayed a gradual decrease in E' through the semimelt state. However, DMA failed to predict that the thermoforming window could be significantly widened by including a few layers of LLDPE. We have demonstrated that the inclusion of 8% of LLDPE in iPP fashioned as 10 thin LLDPE layers broadens the thermoforming window of iPP significantly with no significant reduction in stiffness of the iPP structure. Moreover, such a low level of PE allows these multilayer sheets to be recycled as iPP.

The $iPP_{92}/LLDPE_8$ multilayer sheet displayed a rapid decrease in E' through the semimelt state via DMA, similar to the iPP control. Microscopy revealed that layer integrity is maintained during the thermoforming process. SEM images were utilized to estimate the local strains occurring in the sheet during thermoforming while local stresses were estimated from the cone geometry and the vacuum level applied. The reduction in σ_y, below the local stress estimate, with the addition of LLDPE to the multilayer sheets explained the widened thermoforming window at temperatures less than 160 °C. The introduction of immiscible interfaces when layered with iPP and the resulting interfacial tension drastically reduced sag deflection during heating at temperatures greater than 160 °C to further widen the thermoforming window of the multilayer sheet. Good adhesion between iPP and LLDPE layers in the solid state was ensured by selecting metallocene grades.

■ ASSOCIATED CONTENT

Supporting Information

The Supporting Information is available free of charge at https://pubs.acs.org/doi/10.1021/acsami.2c08586.

Form dimensions, sheet temperature measurements, tensile properties of iPP and multilayer sheet, thermal/mechanical calculations, thermoforming motion study, and sag visualization experiments (PDF)

■ AUTHOR INFORMATION

Corresponding Author

Alex M. Jordan − *Plastics Engineering, University of Wisconsin—Stout, Menomonie, Wisconsin 54751, United States;* orcid.org/0000-0002-9331-6535; Phone: (715) 232-5463; Email: jordanal@uwstout.edu

Authors

Laryssa Meyer − *Plastics Engineering, University of Wisconsin—Stout, Menomonie, Wisconsin 54751, United States*

Kyungtae Kim − *Department of Chemical Engineering & Materials Science, University of Minnesota, Minneapolis, Minnesota 55454, United States;* Present Address: Center for Integrated Nanotechnologies, Los Alamos National Laboratory, Los Alamos, New Mexico 87544, United States

Bongjoon Lee − *Department of Chemical Engineering & Materials Science, University of Minnesota, Minneapolis, Minnesota 55454, United States*

Frank S. Bates − *Department of Chemical Engineering & Materials Science, University of Minnesota, Minneapolis, Minnesota 55454, United States;* orcid.org/0000-0003-3977-1278

Christopher W. Macosko − *Department of Chemical Engineering & Materials Science, University of Minnesota, Minneapolis, Minnesota 55454, United States;* orcid.org/0000-0002-2892-3267

Complete contact information is available at: https://pubs.acs.org/10.1021/acsami.2c08586

Author Contributions

A.M.J. planned and coordinated coextrusion runs and thermoforming trials, analyzed thermoforming data, collected and analyzed mechanical data, performed calculations, supervised participants, and prepared manuscript. L.M. conducted thermoforming temperature and crush strength trials. K.K. and B.L. prepared multilayer films. C.W.M. and

https://doi.org/10.1021/acsami.2c08586
ACS Appl. Mater. Interfaces XXXX, XXX, XXX−XXX

F.S.B. participated in the initial planning of the research, supervised several of the participants, and edited the manuscript.

Notes

The authors declare no competing financial interest.

■ ACKNOWLEDGMENTS

The authors thank Dr. Hanseung Lee for his assistance with SEM imaging. They also thank Dr. Olivier Lhost and Dr. Yves Trolez of TotalEnergies for their helpful discussions on the thermoforming process. This research was supported by a grant from TotalEnergies with partial support by the Industrial Partnership for Research in Interfacial & Materials Engineering (IPRIME). Polymers were graciously provided by TotalEnergies and ExxonMobil Corporation. Parts of this work were carried out in the Characterization Facility, University of Minnesota, a member of the NSF-funded Materials Research Facilities Network (www.mrfn.org) via the MRSEC program. The Hitachi SU8320 cryoSEM and cryospecimen preparation system were provided by NSF MRI DMR-1229263.

■ REFERENCES

(1) Grand View Research. *Plastic Packaging Market Size, Share & Trends Analysis Report By Product (Flexible, Rigid), By Technology (Extrusion, Thermoforming), By Application (Food & Beverages, Pharmaceuticals), And Segment Forecasts, 2021−2028*; Grand View Research, Inc.: San Francisco, 2021.

(2) Lau, H. C.; Bhattacharya, S. N.; Field, G. J. Melt Strength of Polypropylene: Its Relevance to Thermoforming. *Polym. Eng. Sci.* **1998**, *38*, 1915−1923.

(3) Lau, H. C.; Bhattacharya, S. N.; Field, G. J. Influence of Rheological Properties on the Sagging of Polypropylene and ABS Sheet for Thermoforming Applications. *Polym. Eng. Sci.* **2000**, *40*, 1564−1570.

(4) Macauley, N. J.; A Harkin-Jones, E. M.; Murphy, W. R. The Influence of Nucleating Agents on the Extrusion and Thermoforming of Polypropylene. *Polym. Eng. Sci.* **1998**, *38*, 516−523.

(5) Li, S.; Xiao, M.; Guan, Y.; Wei, D.; Xiao, H.; Zheng, A. A Novel Strategy For The Preparation of Long Chain Branching Polypropylene and the Investigation on Foamability and Rheology. *Eur. Polym. J.* **2012**, *48*, 362−371.

(6) Marathe, D.; Shelar, S.; Mahajan, S.; Ahmad, Z.; Gupta, S.; Kulkarni, S.; Juvekar, V.; Lele, A. Study of Rheology and Plut Assist Thermoforming of Linear and Branched PP Homopolymer and Impact Copolymer. *Int. Polym. Process.* **2019**, *3*, 339−355.

(7) Weng, W.; Markel, E. J.; Dekmezian, A. H. Synthesis of Long-Chain Branched Propylene Polymers via Macromonomer Incorporation. *Macromol. Rapid Commun.* **2001**, *22*, 1488−1492.

(8) Münstedt, H.; Kurzbeck, S.; Stange, J. Advances in Film Blowing, Thermoforming, and Foaming by Using Long-Chain Branched Polymers. *Macromol. Symp.* **2006**, *245−246*, 181−190.

(9) Münstedt, H.; Kurzbeck, S.; Stange, J. Importance of Elongational Properties of Polymer Melts for Film Blowing and Thermoforming. *Polym. Eng. Sci.* **2006**, *46*, 1190−1195.

(10) Gotsis, A. D.; F Zeevenhoven, B. L.; Hogt, A. H. The Effect of Long Chain Branching on the Processability of Polypropylene in Thermoforming. *Polym. Eng. Sci.* **2004**, *44*, 973−982.

(11) Yamaguchi, M.; Suzuki, K. Enhanced Strain Hardening in Elongational Viscosity for HDPE/Crosslinked HDPE Blend. II. Processability of Thermoforming. *J. Appl. Polym. Sci.* **2002**, *86*, 79−83.

(12) Jordan, A. M.; Lee, B.; Kim, K.; Ludtke, E.; Lhost, O.; Jaffer, S. A.; Bates, F. S.; Macosko, C. W. Rheology of Polymer Multilayers: Slip in Shear, Hardening in Extension. *J. Rheol.* **2019**, *63*, 751−761.

(13) Jordan, A. M.; Kim, K.; Soetrisno, D.; Hannah, J.; Bates, F. S.; Jaffer, S. A.; Lhost, O.; Macosko, C. W. Role of Crystallization on Polyolefin Interfaces: An Improved Outlook for Polyolefin Blends. *Macromolecules* **2018**, *51*, 2506−2516.

(14) Chaffin, K. A.; Knutsen, J. S.; Brant, P.; Bates, F. S. High-Strength Welds in Metallocene Polypropylene/Polyethylene Laminates. *Science* **2000**, *288*, 2187−2190.

(15) Chaffin, K. A.; Bates, F. S.; Brant, P.; Brown, G. M. Semicrystalline Blends of Polyethylene and Isotactic Polypropylene: Improving Mechanical Performance by Enhancing the Interfacial Structure. *J. Polym. Sci., Part B: Polym. Phys.* **2000**, *38*, 108−121.

(16) Zhang, G.; Lee, P. C.; Jenkins, S.; Dooley, J.; Baer, E. The Effect of Confined Spherulite Morphology of High-Density Polyethylene and Polypropylene on Their Gas Barrier Properties in Multilayered Film Systems. *Polymer* **2014**, *55*, 4521−4530.

(17) Wang, H.; Keum, J. K.; Hiltner, A.; Baer, E.; Freeman, B.; Rozanski, A.; Galeski, A. Confined Crystallization of Polyethylene Oxide in Nanolayer Assemblies. *Science* **2009**, *323*, 757−760.

(18) Carr, J. M.; Langhe, D. S.; Ponting, M. T.; Hiltner, A.; Baer, E. Confined Crystallization in Polymer Nanolayered Films: A Review. *J. Mater. Res.* **2012**, *27*, 1326−1350.

(19) Lee, P. C.; Park, H. E.; Morse, D. C.; Macosko, C. W. Polymer-Polymer Interfacial Slip in Multilayered Films. *J. Rheol.* **2009**, *53*, 893.

(20) Zhang, J.; Lodge, T. P.; Macosko, C. W. Interfacial Slip Reduces Polymer-Polymer Adhesion During Coextrusion. *J. Rheol.* **2006**, *50*, 41−57.

(21) Throne, J. *Understanding Thermoforming*, 2nd ed.; Carl Hanser Verlag: Munich, 2008.

(22) NASA-Langley. *Buckling of Thin-Walled Truncated Cones*; National Aeronautical and Space Administration: Langley, VA, 1968.

(23) Ebert, C.; Hufenbach, W.; Langkamp, A.; Gude, M. Modelling of Strain Rate Dependent Deformation Behaviour of Polypropylene. *Polym. Test.* **2011**, *30*, 183−187.

(24) Stehling, F. C.; Meka, P. Heat Sealing of Semicrystalline Polymer Films. II. Effect of Melting Distribution on Heat-Sealing Behavior of Polyolefins. *J. Appl. Polym. Sci.* **1994**, *51*, 105−119.

(25) Rosenzweig, N.; Narkis, M.; Tadmor, Z. Wall Thickness Distribution in Thermoforming. *Polym. Eng. Sci.* **1979**, *19*, 946−951.

(26) Throne, J. L. Guidelines for Thermoforming Part Wall Thickness. *Polym.-Plast. Technol. Eng.* **1991**, *30*, 685−700.

(27) Association of Plastics Recyclers, PE Film Design Guidance. https://plasticsrecycling.org/pe-film-design-guidance (accessed January 23, 2022).

https://doi.org/10.1021/acsami.2c08586
ACS Appl. Mater. Interfaces XXXX, XXX, XXX−XXX